Heliyon 10 (2024) e34932

Contents lists available at ScienceDirect

Heliyon

journal homepage: www.cell.com/heliyon

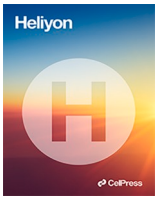

Research article

Aloe-emodin alleviates inflammatory bowel disease in mice by modulating intestinal microbiome homeostasis via the IL-4/IL-13 axis

Dong Yang [*,1], Tingrui Ge [1], Jingyi Zhou, Huazhuan Li, Yonggang Zhang [**]

Department of Anorectal Surgery, The First People's Hospital of Lianyungang, NO.6 Zhenhua East Road, Haizhou District, Lianyungang, 222061, Jiangsu, China

ARTICLE INFO

Keywords:
Aloe-emodin
Inflammatory bowel disease
Intestinal microbiome
IL-4/IL-13 pathway

ABSTRACT

Introduction: Inflammatory bowel disease (IBD) is a global health concern. Aloe-emodin (AE) has diverse pharmacological benefits, including anti-inflammatory effects. However, its role in IBD remains unclear, prompting our investigation of its regulatory effects and mechanisms in an IBD mouse model.

Methods: We studied the therapeutic efficacy of AE in alleviating symptoms and modulating cytokine secretion in a murine model of dextran sulfate sodium (DSS)-induced colitis. BALB/c mice were administered DSS to induce colitis and were subsequently treated with varying doses of AE. Changes in body weight, fecal lipocalin-2 (LCN2) levels, colon tissue histology, and serum cytokine concentrations were evaluated to assess the effects of AE treatment. Additionally, 16 S rRNA sequencing was used to analyze alterations in the composition of the gut microbiota following AE intervention. Finally, the database was used to analyze the signaling pathways associated with IBD in AE and to detect the expression levels of interleukin (IL)-4 pathway using real-time quantitative reverse transcription PCR. Exogenous IL-4 was used in rescue experiments to observe its effects on the disease process of IBD under AE regulation.

Results: AE treatment resulted in a dose-dependent mitigation of weight loss, reduction in fecal LCN2 levels, and amelioration of histological damage in DSS-induced colitis in mice. The levels of superoxide dismutase and catalase increased, whereas malondialdehyde decreased following AE treatment, indicating a dose-dependent alleviation of colitis symptoms. Furthermore, AE administration attenuated the secretion of pro-inflammatory cytokines, including IL-17, tumor necrosis factor-alpha (TNF-α), and chemokine ligand 1, while promoting the expression of anti-inflammatory cytokines IL-4 and IL-13. Analysis of the gut microbiota revealed that AE effectively suppressed the overgrowth of colitis-associated bacterial species and restored microbial homeostasis. Finally, we found that overexpression of IL-4 was able to reverse the therapeutic effect of AE for DSS-induced IBD.

Conclusion: AE shows promise in alleviating colitis severity, influencing inflammatory cytokines, and modulating the gut microbiota in an IBD mouse model via the IL-4/IL-13 pathway, suggesting its potential as a natural IBD remedy.

* Corresponding author.
** Corresponding author. Department of Anorectal surgery, The First People's hospital of Lianyungang,NO.6 Zhenhua East Road, Haizhou District, Lianyungang, 222061, Jiangsu, China.
E-mail addresses: dongyang20122023@163.com (D. Yang), zyg10812@163.com (Y. Zhang).
[1] These authors contributed equally to this work.

https://doi.org/10.1016/j.heliyon.2024.e34932
Received 6 April 2024; Received in revised form 11 July 2024; Accepted 18 July 2024
Available online 22 July 2024

1. Introduction

Inflammatory bowel disease (IBD), encompassing ulcerative colitis and Crohn's disease, is a challenging chronic inflammatory disorder of the gastrointestinal tract [1,2]. Although historically less prevalent in China than in developed Western nations [3], recent years have witnessed an increase in its incidence and prevalence within the country. Projections indicate that China may harbor more than 1.5 million IBD cases by 2025 [4]. Despite its relatively low mortality rate, IBD required lifelong management, with severe cases often culminating in surgery [5]. Moreover, emerging research underscores the heightened risk of colorectal and pancreatic cancers among patients with IBD [6,7], emphasizing the critical need for effective preventive and therapeutic strategies.

The intricate pathogenesis of IBD involves immune responses, environmental influences, genetic predispositions, and interactions within the gut microenvironment, particularly with intestinal microbiota [8,9]. Key studies have elucidated the pivotal role of various immune cell populations, including macrophages, T cells, B cells, dendritic cells, and mesenchymal stem cells, distributed throughout the intestinal milieu [10,11]. In particular, T cell subsets such as T helper cell 17 (Th17), T helper cell 9 (Th9), and regulatory T cells have emerged as crucial players in IBD pathophysiology, with Th17 cells exhibiting dual roles in maintaining intestinal homeostasis and exacerbating inflammation under pathological conditions [12,13]. Dysbiosis within the intestinal microbiota, which is marked by reduced diversity and altered composition, significantly contributes to mucosal damage and inflammation in patients with IBD [14]. Consequently, interventions targeting immune cell dysregulation and microbiota imbalance hold promise for mitigating the progression of IBD.

Current therapeutic approaches predominantly rely on aminosalicylic acid preparations, glucocorticoids, immunosuppressants, and biologics [15]. However, their efficacy is affected by adverse effects, including drug resistance and perturbations in the gut flora, which often hamper long-term outcomes. In contrast, Traditional Chinese Medicine (TCM) has garnered attention for its holistic approach and favorable patient acceptance, particularly in East Asian countries [16,17]. By leveraging multiple targets with minimal adverse reactions, TCM offers tailored treatment regimens that exhibit considerable efficacy in alleviating symptoms, promoting remission, and enhancing the quality of life of patients [18,19]. However, despite promising clinical outcomes of TCM, research elucidating the specific anti-inflammatory and immunomodulatory mechanisms of its constituents is still in its nascent stage. Thus, investigating the immunoregulatory and anti-inflammatory properties of TCM monomers is paramount for elucidating their pharmacological effects on IBD.

Aloe-emodin (AE) is a natural anthraquinone derived from medicinal herbs such as Aloe vera and is commonly found in the roots and rhizomes of various plants [20]. Its molecular weight is 270.24 g/mol and it exists in a solid form. It has garnered attention for its purported anti-inflammatory and anti-neoplastic properties [21,22]. In addition, AE has antiviral activity against influenza A virus [22]. Despite its demonstrated efficacy in various models [23,24], its potential in alleviating IBD-related inflammation and modulating intestinal microbiota remains largely unexplored. This study aimed to elucidate the pharmacological effects of AE on IBD and lay the groundwork for its clinical application.

Among the inflammatory factors secreted by helper T cells, IL-4/IL-13 has garnered significant attention. The IL-4/IL-13 pathway has been implicated in inflammatory diseases [25,26]. A study has indicated IL-13 involvement in the pathogenesis of myelofibrosis, suggesting inhibition of the IL-4/IL-13 pathway as a potential therapeutic strategy against this condition [27]. Currently, dupilumab is used as an IL-4/IL-13 blocker for the treatment of several type 2 inflammation [28]. In addition, a previous research has highlighted the IL-4/IL-13 signaling axis as a potent yet targetable profibrotic mechanism in the lower urinary tract [29]. However, the role of the IL-4/IL-13 pathway in IBD remains unexplored. Hence, this study aimed to investigate whether AE affects the course of IBD via modulation of the IL-4/IL-13 axis.

2. Materials and methods

2.1. Animal model and treatments

BALB/c mice (Vital River Laboratories, Beijing, China) aged 6–8 weeks were used to establish the experimental model. Model construction has been reported in previous studies [30]. The study included 15 mice initially which were divided into the following groups. Negative control group (n = 3) which received the same volume of normal saline via gavage as the treatment groups. Dextran sulfate sodium (DSS)-induced colitis group (n = 12) in which colitis was induced by administering sterile drinking water containing 3 % DSS for 7 days. When the mice exhibited weight loss, loose stools, diarrhea, bloody stools, and ulcers, the DSS treatment was deemed effective, confirming the successful establishment of the animal model. This group was further subdivided into positive control group (DSS-only, n = 3): These mice continued to receive DSS without any further treatment. AE treatment groups: These groups received daily intragastric administration of AE (HY–N0189; MCE, Monmouth Junction, NJ, USA), dissolved in 20 % PEG400 in saline according to the manufacturer's instructions, from days 8–15. The AE treatment groups included: high-dose AE group (n = 3, 50 mg/kg/day), Middle-dose AE group (n = 3, 10 mg/kg/day) and Low-dose AE group (n = 3, 5 mg/kg/day). Mice were weighed daily throughout the experiment to monitor changes in body weight. Upon completion of the experiment, the mice were euthanized via excess CO_2 inhalation, followed by dissection. The mesenteric lymph node, the largest lymph node in the mouse body, is shaped like an earthworm and extends through the fatty tissue of the mesentery. To locate and remove this lymph node, we first identified the vermiform appendix. From there, we traced along the mesentery upstream and carefully cut open the mesenteric tissue. This allowed for the removal of the mesenteric lymph node. Colorectal tissues were collected approximately 1–2 cm away from the rectum. Colorectal tissues, approximately 1–2 cm away from the rectum, were dissected and divided into two parts, one part was placed in 4 %

paraformaldehyde fixative for subsequent pathological testing, and one part was placed in a −80 °C refrigerator for investigating the expression level of IL-4 and IL-13 and testing of proteins molecules and other assays. Blood was collected by ocular phlebotomy for subsequent testing. After collection, the blood was allowed to stand at room temperature for 30 min before being centrifuged at 4 °C for 10 min at 2000 rpm to obtain serum. For fecal samples used in the analysis of intestinal flora, we used the natural defecation method. One day before the end of the experiment, the mice were placed into a fecal collector or an empty mouse cage and allowed to defecate naturally. Feces were collected promptly to avoid contamination. Once sufficient feces were collected, the mice were promptly returned to their cages. The collected fecal samples were then used for DNA extraction. The amplified DNA fragments were sequenced (Beijing Genomics institute), and the resulting sequences were analyzed to identify and classify the bacterial taxa present in the samples for 16 S ribosomal DNA identification. In another set of experiments, we again established DSS-induced colitis mice (n = 15) following the procedure described above. After successful modeling of DSS-induced colitis, we evaluated the effects of IL-4 in these colitis mice by dividing them into five groups: Negative control group (n = 3), DSS group without any treatment (n = 3), negative control group pcDNA-NC: These mice received a tail vein injection of a control plasmid (pcDNA-NC, n = 3). Positive control group (pcDNA-NC + AE, n = 3): These mice received daily intragastric administration of AE as described above for first set of experiment. After AE treatment, they received an equal amount of control plasmid (pcDNA-NC) via tail vein injection. Treatment group (pcDNA-IL-4 + AE, n = 3): These AE-treated mice received a tail vein injection of 2×10^{1o} adenoviral particles carrying the mouse IL-4 gene.

Adenovirus particles were obtained from the VectorBuilder software. Body weight of these mice was recorded daily. At the end of the experiment, intestinal tissues were collected and placed in 4 % paraformaldehyde fixative for subsequent pathological testing. The animal experimental protocols were approved by the Animal Ethics Committee of the First People's Hospital of Lianyungang (approval No. KD07230005).

2.2. Enzyme-linked immunosorbent assay (ELISA)

Serum samples were obtained from the mice in each experimental group after 15 days of treatment. The levels of IL-17 (ab100702; Abcam, Cambridge, UK), tumor necrosis factor-alpha (TNF-α) (E-MSEL-M0002; Elabscience, Houston, TX, USA), and chemokine (C-X-C motif) ligand 1 (CXCL1) (ab213859; Abcam) were quantified using commercially available enzyme-linked immunosorbent assay (ELISA) kits, following the manufacturer's instructions. Additionally, fecal samples collected on day 15 were used for the detection of lipocalin-2 (LCN2) using an ELISA kit (RK-KOA0515; Rockland, Limerick, PA, USA). Colonic tissues harvested on day 15 were assessed for total superoxide dismutase (T-SOD), catalase (CAT), and malondialdehyde (MDA) levels. The levels of these oxidative stress markers were determined using kits obtained from Solarbio (Beijing, China) and Abbkine (Atlanta, GA, USA) following the manufacturer's instructions.

2.3. Hematoxylin and eosin (H&E) staining and scoring

Colon tissue samples, approximately 1–2 cm away from the rectum, were excised and immediately fixed in 40 g/L paraformaldehyde solution. For histological examination, sections of the fixed colon tissue were processed for H&E staining using a H&E staining kit (C0105S; Beyotime, Jiangsu, China). Briefly, tissue sections were deparaffinized in xylene, rehydrated through a graded series of ethanol solutions, and stained with hematoxylin to visualize the cell nuclei. Subsequently, the sections were counterstained with eosin to visualize cytoplasmic structures. After staining, the sections were dehydrated in ethanol, cleared in xylene, and mounted with a coverslip using a mounting medium.

2.4. Flow cytometry

Mouse mesenteric lymph node cells were gently removed from the mesenteric lymph node tissues of mice using ethylenediaminetetraacetic acid. The mesenteric lymph node tissues were then subjected to enzymatic digestion using a mixture composed of type A collagenase (1.5 g/L), type I DNase (0.05 g/L), and neutral protease (2 g/L) at 37 °C for 45 min, facilitating the generation of a single-cell suspension. The resulting single cells were subsequently diluted to a concentration of 4×10^6 cells/mL in RPMI 1640 medium supplemented with 10 % fetal bovine serum (FBS). Next, 500 μL of the cell suspension was aliquoted into each well of a 24-well plate, followed by the addition of 2 μL of Cell Activation Cocktail (Brefeldin A) to each well. The cells were then cultured in a 37 °C incubator with CO_2 for 4.5 h to induce stimulation. The stimulated cells were carefully collected and fixed with a Fixation Buffer (420801; BioLegend, San Diego, CA, USA) for 20 min at room temperature. Subsequently, the fixed cells were re-suspended in 1 ml of 1 × Permeabilization Wash Buffer (421002; BioLegend). Specific fluorescently labeled antibodies, including FITC anti-mouse CD45 (147709; BioLegend) and APC anti-mouse IL-17 (506915; BioLegend), were added to the cell suspension and incubated at room temperature for 30 min in the dark, enabling the detection of immune cell markers and cytokines by flow cytometry.

2.5. TUNEL assay

Colon tissue samples were harvested from mice and immediately fixed in 40 g/L paraformaldehyde solution. Subsequently, paraffin sections of fixed tissues were prepared according to the manufacturer's instructions using an apoptosis detection kit (C1091; Beyotime). Briefly, terminal deoxynucleotidyl transferase was used to label DNA strand breaks in the colon tissue sections. The incorporation of fluorescein-labeled nucleotide polymers was visualized using fluorescence microscopy, allowing for the detection of apoptotic cells.

2.6. Real-time quantitative reverse transcription PCR (RT-qPCR)

Total RNA was extracted from the colon tissue of control, DSS-induced colitis, and DSS + AE mice and purified using TRIzol reagent. The integrity and purity of the RNA were verified using UV spectrophotometry and formaldehyde denaturing electrophoresis. For reverse transcription, 1 μg of total RNA was used, and cDNA synthesis was achieved utilizing AMV reverse transcriptase. To quantify gene expression changes relative to the internal reference gene GAPDH, the $2^{-\Delta\Delta Ct}$ method was used to normalize gene expression levels across different samples. The results were obtained using three independent biological replicates to ensure reliability and reproducibility. The primer sequences used for amplification were as follows: mIL-4 forward: TTGAACGAGGTCACAGGAGAAG, reverse: CCTTGGAAGCCCTACAGACG. mIL-13, forward: AACGGCAGCATGGTATGGAGTG, reverse: TGGGTCCTGTAGATGGCATTGC; β-actin forward: CCAGCCTTCCTTCTTGGGTAT, reverse: AGAGGTCTTTACGGATGTCAACG.

2.7. Bioinformatics analysis

To identify potential targets associated with AE and colitis, a comparative analysis was performed using the Comparative Toxicogenomics Database (CTD; https://ctdbase.org/) and gene ontology (GO; https://geneontology.org/). The CTD was used to retrieve genes associated with both AE and colitis. This database integrates curated data on chemical-gene/protein interactions, chemical-disease, and gene-disease relationships from the literature. GO analysis was conducted to categorize and annotate the identified genes based on their biological processes, molecular functions, and cellular components. This analysis provided insights into the functional roles and biological pathways associated with the identified genes. Comparative analysis of AE and colitis using CTD and GO analyses facilitated the identification of potential targets and pathways involved in the therapeutic effects of AE on colitis.

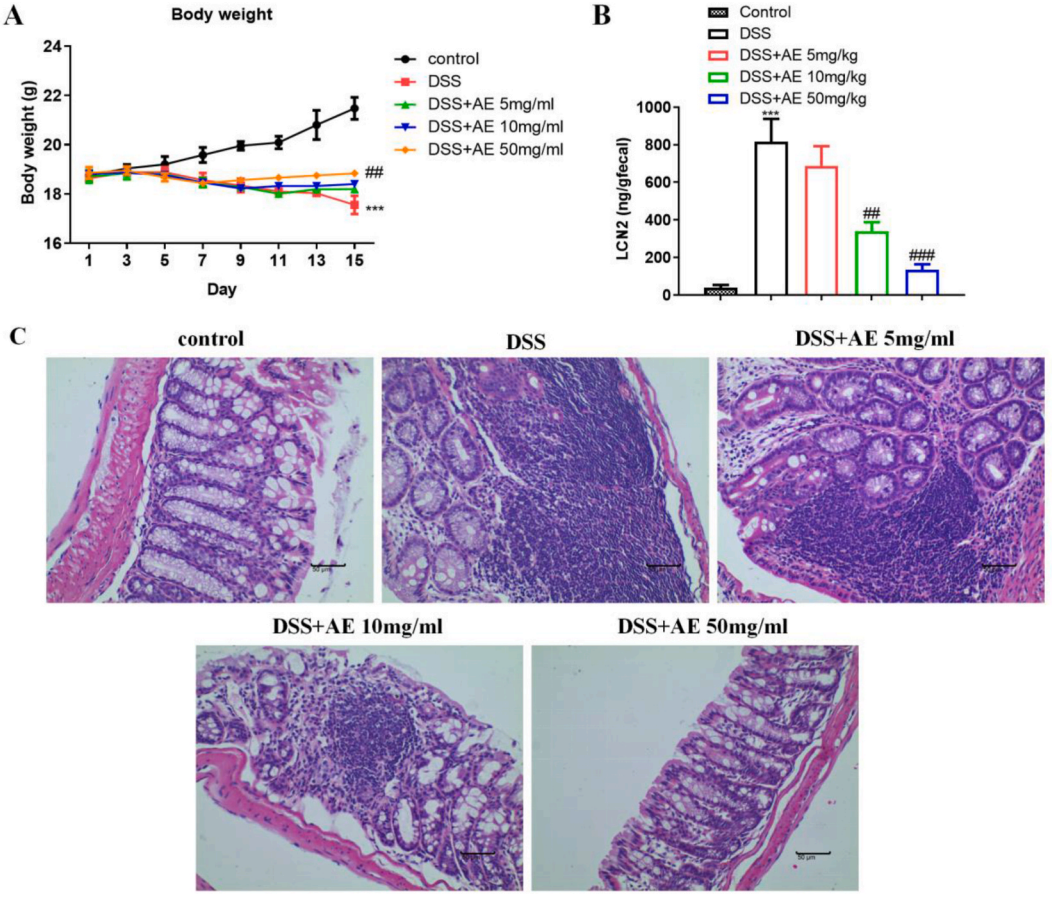

Fig. 1. ***AE alleviates mice colitis induced by DSS. A**: Changes in body weights of mice were monitored following treatment with different doses of AE in a mouse model of colitis induced by DSS. **B**: Intestinal inflammation marker LCN2 in feces. Levels of LCN2 in fecal samples collected from mice were measured as a marker of intestinal inflammation. **C**: H&E staining of colon tissue sections. Histological evaluation of colon tissue slices stained with H&E to assess tissue damage and inflammation. Representative images are shown. Data are shown as mean ± SD, ***P < 0.001: compared with control group; ##P < 0.01 and ###P < 0.001: compared with DSS group. Representative results from one out of three independent experiments.*

Table 1
Weight changes in control, DSS induced, and AE treated mice (g).

	Control	DSS	DSS + AE 5 mg/ml	DSS + AE 10 mg/ml	DSS + AE 50 mg/ml
1 day	18.76 ± 0.15	18.63 ± 0.14	18.70 ± 0.25	18.82 ± 0.08	18.86 ± 0.23
3 day	19.04 ± 0.16	18.89 ± 0.14	18.84 ± 0.25	18.86 ± 0.09	18.95 ± 0.17
5 day	19.20 ± 0.32	18.88 ± 0.21	18.81 ± 0.05	18.76 ± 0.12	18.68 ± 0.16
7 day	19.58 ± 0.31	18.57 ± 0.30	18.46 ± 0.18	18.47 ± 0.06	18.44 ± 0.11
9 day	19.96 ± 0.18	18.34 ± 0.27	18.29 ± 0.12	18.22 ± 0.04	18.56 ± 0.09
11 day	20.09 ± 0.25	18.10 ± 0.11	18.01 ± 0.07	18.32 ± 0.12	18.66 ± 0.08
13 day	20.80 ± 0.59	18.03 ± 0.09	181.19 ± 0.05	18.32 ± 0.14	18.75 ± 0.05
15 day	21.48 ± 0.45	17.56 ± 0.37	18.02 ± 0.04	18.40 ± 0.13	18.83 ± 0.07
P value		0.000	0.039	0.020	0.004

2.8. Statistical analysis

To assess the differences among experimental groups, Student's t-test or analysis of variance (ANOVA) was performed, followed by Tukey's post-hoc test for multiple comparisons. All statistical analyses were conducted with a minimum of three independent replicates to ensure the robustness and reliability of the results. Data are expressed as mean ± standard error (SE). Statistical significance was defined as $P < 0.05$. GraphPad Prism (version 6.0; GraphPad Prism Software, La Jolla, CA, USA) was used for all statistical analyses, facilitating the accurate interpretation of the data and identification of significant differences between groups.

3. Results

3.1. Therapeutic effects of AE on DSS-induced colitis in mice

We investigated the impact of AE treatment on mouse weight loss and the levels of LCN2 in fecal samples as a marker of intestinal inflammation. Following the induction of colitis with DSS, DSS-mice exhibited significant weight loss (mean ± SD: 17.56 ± 0.37 g on day 15), indicative of severe disease progression (Fig. 1A, Table 1, P = 0.000). However, AE intervention resulted in a dose-dependent alleviation of weight loss in the treatment groups. Notably, mice administered higher doses of AE (10 and 50 mg/kg) demonstrated a more pronounced improvement in body weight (mean ± SD: 18.40 ± 0.13 g and 18.83 ± 0.07 g on day 15, respectively) than those administered a lower dose (5 mg/kg) (Fig. 1A and Table 1, P = 0.020 and P = 0.004).

Because LCN2 serves as a sensitive marker of intestinal inflammation [31], we assessed its levels in fecal samples collected from mice using ELISA. Consistent with the severity of colitis, the DSS group showed markedly elevated LCN2 levels (mean ± SD: 817.00 ± 121.20 ng/g fecal content), while AE treatment led to a dose-dependent reduction in fecal LCN2 content, suggesting the mitigation of intestinal inflammation in response to AE intervention (mean ± SD: 339.47 ± 48.15 ng/g and 135.72 ± 27.71 ng/g for 10 and 50 mg/kg doses, respectively) (Fig. 1B–Table 2, P = 0.003 and P = 0.000). Histological examination of colon tissue slices revealed severe colonic ulcers and tissue damage in mice in the DSS group, characterized by hyperemia, edema, disorganized epithelial cells, and disruption of the epithelial barrier. Conversely, mice treated with AE exhibited a significant reduction in histological damage compared to the DSS group. This reduction was dose-dependent and correlated with improvements in epithelial cell organization, normalization of crypt morphology, and reduced infiltration of inflammatory cells (Fig. 1C). Overall, AE treatment mitigated weight loss, reduced LCN2 levels, and ameliorated histological damage in the mouse model of DSS-induced colitis.

3.2. AE reduced inflammatory cytokines in the DSS-induced colitis in mice

Next, we investigated the effects of AE on the levels of inflammatory cytokines in a mouse model of DSS-induced colitis. Colitis is associated with the production of inflammatory cytokines, such as TNF-α and IL-17. Following DSS induction, there was a significant increase in the levels of TNF-α (mean ± SD: 333.26 ± 28.87 pg/ml) and IL-17 (mean ± SD: 443.68 ± 23.88 pg/ml) in the serum of mice (Fig. 2A, Table 3, P = 0.000). However, AE treatment in a dose-dependent manner effectively reduced the production of TNF-α (mean ± SD: 213.10 ± 12.70 pg/ml and 142.22 ± 16.66 pg/ml for 10 and 50 mg/kg doses, respectively) and IL-17 (mean ± SD: 305.58 ± 22.43 pg/ml and 191.59 ± 26.05 pg/ml for 10 and 50 mg/kg doses, respectively) (Fig. 2A–Table 3, P = 0.003 and P = 0.000).

Given the ability of AE to reduce granulocyte and monocyte infiltration in various diseases [32–34], we also measured the serum levels of CXCL1, a chemokine involved in recruiting these immune cells. AE treatment led to a reduction in CXCL1 secretion, compared with DSS group (mean ± SD: 1283.41 ± 92.14 pg/ml and 563.47 ± 101.14 pg/ml for 10 and 50 mg/kg doses, respectively)

Table 2
The content of LCN2 in control, DSS induced, and AE treated mice (ng/gfecal).

	Control	DSS	DSS + AE 5 mg/kg	DSS + AE 10 mg/kg	DSS + AE 50 mg/kg
	39.84 ± 13.62	817.00 ± 121.20	687.78 ± 104.60	339.47 ± 48.15	135.72 ± 27.71
P value		0.000	0.235	0.003	0.000

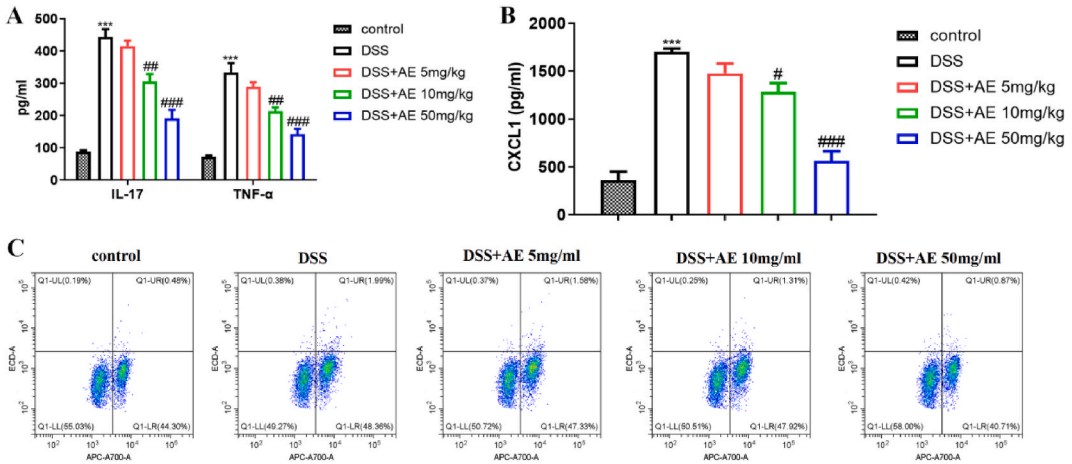

Fig. 2. AE reduces the inflammatory cytokines in the DSS-induced colitis in mice. A: Inflammatory cytokines IL-17 and TNF-α in serum detected by ELISA. **B:** Chemokines CXCL1 in serum detected by ELISA. **C:** Th17 cells in mesenteric lymph nodes detected by Flow cytometry. Data are shown as mean ± SD, ***P < 0.001: compared with control group; #P < 0.05, ##P < 0.01 and ###P < 0.001: compared with DSS group. Representative results from one out of three independent experiments.

Table 3
The concentration of IL-17 and TNF-α in control, DSS induced, and AE treated mice (pg/ml).

	Control	DSS	DSS + AE 5 mg/kg	DSS + AE 10 mg/kg	DSS + AE 50 mg/kg
IL-17	87.97 ± 4.31	443.68 ± 23.88	414.71 ± 17.69	305.58 ± 22.43	191.59 ± 26.05
P value		0.000	0.167	0.002	0.000
TNF-α	72.28 ± 4.49	333.26 ± 28.87	289.22 ± 14.32	213.10 ± 12.70	142.22 ± 16.66
P value		0.000	0.077	0.003	0.000

Table 4
The concentration of CXCL1 in control, DSS induced, and AE treated mice (pg/ml).

	Control	DSS	DSS + AE 5 mg/kg	DSS + AE 10 mg/kg	DSS + AE 50 mg/kg
	360.78 ± 90.52	1701.68 ± 33.90	1476.73 ± 101.69	1283.41 ± 92.14	563.47 ± 101.14
P value		0.000	0.022	0.002	0.000

(Fig. 2B–Table 4, P = 0.002 and P = 0.000), which correlated with decreased infiltration of granulocytes and monocytes in the colon. Further analysis of immune cells in the mouse mesenteric lymph nodes revealed that AE treatment reversed the inflammation-induced increase in Th17 (CD4+IL-17 A+) cells. This observation provides an insight into the mechanism by which AE reduces serum IL-17 levels (Fig. 2C). Overall, AE treatment attenuates the production of inflammatory cytokines, including TNF-α and IL-17, in a mouse model of DSS-induced colitis. Moreover, AE reduced serum CXCL1 levels and reversed the increase in Th17 cells in mesenteric lymph nodes.

3.3. AE restrains oxidative stress and improves intestinal mucosa barrier in the DSS-induced colitis in mice

Oxidative stress plays a pivotal role in the inflammatory response observed in colitis [35], with its excessive presence causing damage to the intestinal mucosal barrier function and exacerbating inflammation. To elucidate the potential of AE in mitigating oxidative stress and enhancing intestinal mucosal integrity, we assessed the effect of various doses of AE on colon cell apoptosis using the TUNEL assay and measured the concentrations of oxidative stress markers, including total antioxidant capacity, T-SOD, CAT, and MDA, in the colon tissues of mice using ELISA. Our results revealed that AE treatment led to a dose-dependent increase in T-SOD (mean ± SD: 108.44 ± 9.45 U/ml and 129.63 ± 7.23 U/ml for 10 and 50 mg/kg doses, respectively) and CAT (mean ± SD: 4.63 ± 0.26 U/mgHb and 6.96 ± 0.39 U/mgHb for 10 and 50 mg/kg doses, respectively) expression levels, and a reduction in MDA levels (mean ± SD: 9.35 ± 0.47 nmol/ml and 6.18 ± 0.47 nmol/ml for 10 and 50 mg/kg doses, respectively), compared with DSS group (Fig. 3A, Table 5, P = 0.007, P = 0.000, and P = 0.000).

Furthermore, AE administration decreased colon epithelial cell apoptosis and conferred protection to the colon mucosa, as evidenced by histological examination (Fig. 3B). Our findings demonstrated that AE effectively restrains oxidative stress and enhances the integrity of the intestinal mucosal barrier in a mouse model of colitis.

3.4. AE regulates the composition of intestinal microbiota in the DSS-induced colitis in mice

To investigate the effects of AE on the intestinal flora of mice, we conducted a comprehensive analysis of bacterial genomic DNA extracted from mouse feces and examined the composition and function of the intestinal microbiota using 16 S rRNA sequencing. Analysis of the Venn diagram revealed no significant differences in the species diversity of the intestinal flora among the control, DSS, and AE-treated groups (50 mg/kg). In total, 594 bacterial communities were identified across the three groups, indicating comparable microbial diversity (Fig. 4A). At the phylum level, the predominant phyla observed in all groups were Firmicutes, Bacteroidetes, Saccharibacteria, Actinobacteria, and Proteobacteria. There were no substantial differences in the abundances of these phyla among the three groups, suggesting a stable microbial composition (Fig. 4B). Further analysis at the species level revealed an increase in the abundance of *Acetatifactor muris* following the induction of colitis. Remarkably, AE (50 mg/kg) treatment effectively suppressed *A. muris* overgrowth, restoring its abundance to normal levels (Fig. 4C). This observation suggested a potential role for AE in inhibiting colitis by modulating the abundance of specific bacterial species. In conclusion, AE treatment modulated the composition of the intestinal microbiota in a mouse model, with a notable effect on specific bacterial species such as *A. muris*.

3.5. AE activated the IL-4/IL-13 pathway in the DSS-induced colitis in mice

Previous studies have indicated that AE possesses anti-inflammatory, antioxidative, and microbiota-regulating properties [23,36]. However, specific targets in colitis remain unclear. Through a comprehensive analysis utilizing the CTD and GO, we identified 12 common targets of AE in colitis that were notably enriched in the IL-4/IL-13 pathway (Fig. 5A and B). Based on this insight, we investigated the expression levels of IL-4 and IL-13 in mouse intestinal tissues. Our results revealed significant upregulation of IL-4 (mean ± SD: 4.37 ± 0.49) and IL-13 (mean ± SD: 3.26 ± 0.33) expression due to DSS, which was effectively reversed by 50 mg/kg

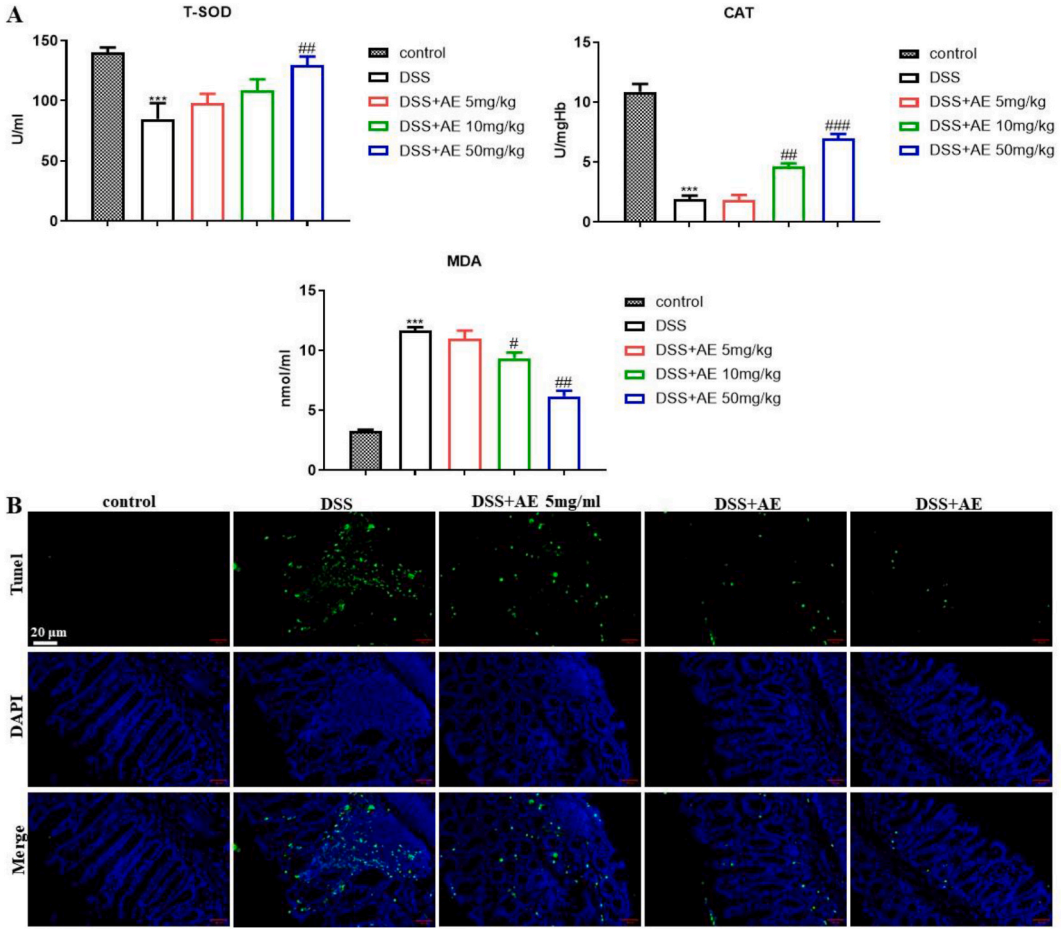

Fig. 3. AE restrains oxidative stress and improves the intestinal mucosa barrier in the DSS-induced colitis in mice. A: Concentrations of T-SOD, CAT, and MDA in the colon were measured in colon tissues of mice treated with variable doses of AE using ELISA. **B:** Assessment of apoptosis in colon tissue slices following treatment with AE using the TUNEL assay. Data are presented as mean ± SD, ***P < 0.001: compared with control group; #P < 0.05, ##P < 0.01 and ###P < 0.001: compared with DSS group. Representative results from one out of three independent experiments.

Table 5
The content of T-SOD, MDA and CAT in control, DSS induced, and AE treated mice.

	Control	DSS	DSS + AE 5 mg/kg	DSS + AE 10 mg/kg	DSS + AE 50 mg/kg
T-SOD (U/ml)	140.20 ± 4.08	84.86 ± 13.17	98.22 ± 7.57	108.44 ± 9.45	129.63 ± 7.23
P value		0.002	0.202	0.065	0.007
CAT (U/mgHb)	10.87 ± 0.65	1.90 ± 0.32	1.86 ± 0.44	4.63 ± 0.26	6.96 ± 0.39
P value		0.000	0.841	0.000	0.000
MDA (nmol/ml)	3.26 ± 0.12	11.69 ± 0.26	1.096 ± 0.71	9.35 ± 0.47	6.18 ± 047
P value		0.000	0.172	0.002	0.000

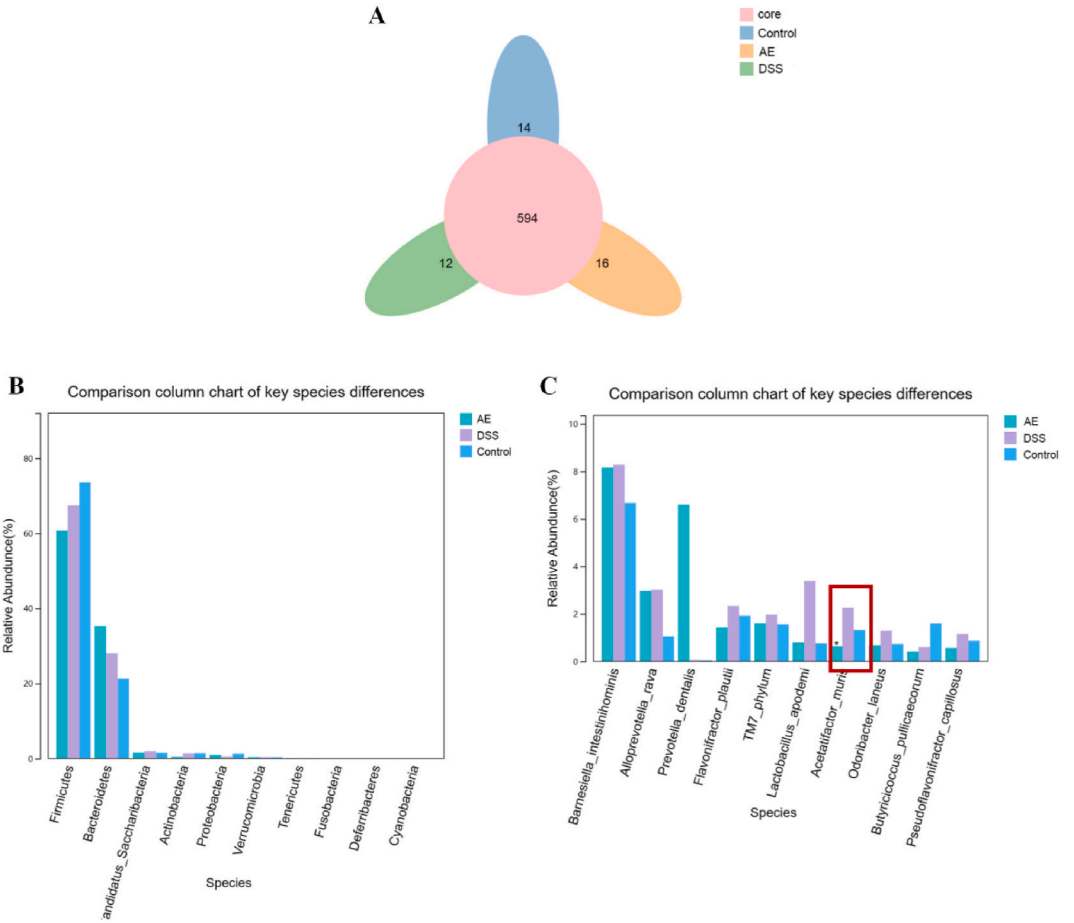

Fig. 4. AE regulates the composition and function of intestinal microbiota in the DSS-induced colitis in mice. **A**: Venn diagram illustrating the overlap of intestinal flora among three groups of mice: control, DSS, and AE-treated (50 mg/kg). The diagram demonstrates comparable species diversity across the groups, with a total of 594 bacterial communities identified. **B**: Abundance maps of phylum classification level depicting the predominant phyla observed in each group, including Firmicutes, Bacteroidetes, Saccharibacteria, Actinobacteria, and Proteobacteria. **C**: Abundance maps of species classification level illustrating the impact of AE treatment (50 mg/kg) on specific bacterial species. Notably, AE treatment (50 mg/kg) effectively suppresses the overgrowth of Acetatifactor muris induced by colitis, restoring its abundance to normal levels. Representative results from one out of three independent experiments.

AE treatment (mean ± SD: 2.30 ± 0.31 for IL-4 and 1.71 ± 0.09 for IL-13) (Fig. 5C–Table 6, P = 0.003 and P = 0.001).

To further validate the involvement of the IL-4/IL-13 pathway, we introduced exogenous IL-4 into mice with colitis through adenovirus intervention via tail vein injection and this group was designated as pcDNA-IL-4. Notably, mice in the exogenous IL-4-treated group lost more weight (mean ± SD: 17.99 ± 0.27 g on day 13) than those in the 50 mg/kg AE-treated group (mean ± SD: 18.71 ± 0.27 g on day 13), suggesting that exogenous IL-4 reversed the therapeutic effect of AE (Fig. 5D–Table 7, P = 0.009). Histological examination of colon tissue sections by H&E staining corroborated these findings, demonstrating that exogenous IL-4 effectively aggravated DSS-induced intestinal injury caused by DSS (Fig. 5E). Our findings suggest that AE exerts anti-inflammatory effects on colitis by inactivating the IL-4/IL-13 pathway.

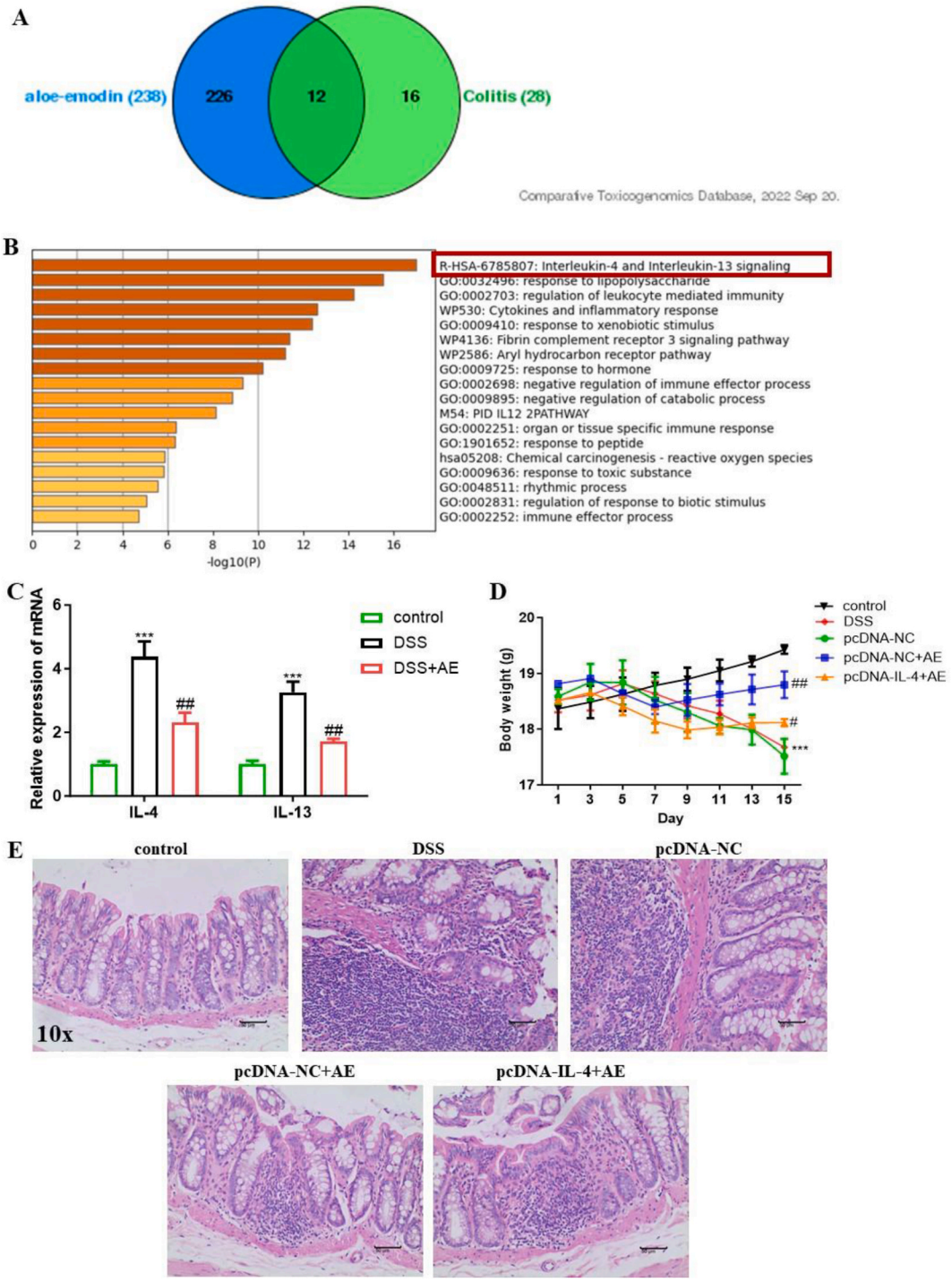

Fig. 5. AE activates the IL-4/IL-13 pathway in the DSS-induced colitis in mice. ***A:*** *Bioinformatics analysis reveals 12 common targets of AE in colitis.* ***B:*** *Gene Ontology analysis illustrates functional annotations of the identified targets.* ***C:*** *RT-PCR analysis demonstrates the expression levels of IL-4 and IL-13 in intestinal tissues of mice before and after* 50 mg/kg AE *treatment.* ***D:*** *Mouse body weight changes following IL-4 intervention in* DSS-induced *colitis mice, indicative of AE-like alleviation of colitis-induced weight loss.* ***E:*** *H&E staining and histological scoring of colon tissue sections depict the protective effect of exogenous IL-4 on DSS-induced intestinal injury. Data are presented as mean ± SD, **P < 0.01 and ***P < 0.001: compared to control group; #P < 0.05 and ##P < 0.01: compared with DSS and pc-DNA-NC + AE group. Representative results from one out of three independent experiments.*

4. Discussion

In recent years, as concerns regarding adverse reactions to conventional medications have increased, there is a pressing need for safer approaches to treat IBD [37]. Natural products have emerged as promising candidates for IBD treatment, with mechanisms involving the repair of the intestinal barrier, regulation of intestinal flora and its metabolites, and modulation of immune responses [38].

Among these natural remedies, AE derived from Aloe vera have garnered significant attention for their multifaceted pharmacological properties. Extensive research has revealed potent anti-inflammatory, antimicrobial, and anticancer effects of AE in various disease models. In sepsis, AE has been shown to activate signaling pathways such as SIRT1 and PI3K/Nrf2/HO-1, resulting in the reduced release of high-mobility group box 1 and decreased mortality [39]. AE has also demonstrated efficacy in overcoming drug resistance in cancer cells, inhibiting cell proliferation and migration, and regulating cell cycle distribution and cellular senescence [40,41]. AE demonstrates growth-suppressive effects on androgen-independent human prostate cancer DU145 cells by inhibiting the Wnt/β-catenin signaling pathway [41]. Additionally, it regulates cell cycle distribution and cellular senescence in human prostate cancer LNCaP cells [42]. Moreover, AE prevents several Huntington's disease-like symptoms through the inhibition of the CaMKII/Smad and TGF-β1/Smad signaling pathways in mice [43]. Notably, AE exhibit greater potency than emodin in terms of cell viability, migration, and MAPK gene expression levels in healthy fibroblastic skin cells [44]. Furthermore, AE demonstrated antimicrobial efficacy *in vitro* and mediated photodynamic therapy against antibiotic-resistant *Pseudomonas aeruginosa* [45].

In the context of IBD, AE has exhibited promising therapeutic potential as evidenced by its ability to attenuate intestinal inflammation, reduce oxidative stress, and modulate the composition of the gut microbiota. Studies have highlighted the capacity of AE to mitigate cardiac inflammation induced by a high-fat diet, attenuate sepsis-induced systemic inflammation, and alleviate lipopolysaccharide-induced inflammation via various signaling pathways [32,46,47]. Furthermore, AE has been reported to alleviate oxidative stress, cognitive impairment, and inflammation in D-galactose-induced models by mediating the ERK, p38, and NF-κB signaling pathways [48]. Overall, AE demonstrated multifaceted therapeutic properties, ranging from anti-inflammatory and antioxidative effects to the modulation of intestinal flora, suggesting its potential as a promising candidate for the treatment of IBD and other inflammatory conditions.

In this study, we aimed to explore the therapeutic potential of AE in IBD using both *in vitro* and *in vivo* experiments. Our findings corroborate those of previous studies demonstrating the ability of AE to reduce inflammatory cytokine secretion via the IL-4/IL-13 pathway, mitigate intestinal immune cell infiltration, and alleviate oxidative stress. Notably, our study also revealed the impact of AE on the composition of the intestinal flora, particularly its ability to suppress the overgrowth of *A. muris*, a bacterium associated with exacerbating colitis. These findings highlighted AE as a promising therapeutic agent for IBD and offered insights into its multifaceted mechanisms of action.

A. muris, initially isolated from the gut of obese mice [49], has been implicated in various studies on its impact on health. Specifically, Lee et al. found that oral administration of *A. muris* exacerbated DSS-induced colitis [50], whereas reports by Wang et al. linked it to adverse effects in acute liver failure [51]. Conversely, Kübeck et al. suggested a role for *A. muris* in regulating obesity by enhancing the intestinal absorption of dietary fats [52]. Despite these findings, the precise regulatory mechanisms of *A. muris* in the gut remain unknown. Previous studies have highlighted its involvement in the production of acetate and butyrate, which modulate inflammatory responses and insulin sensitivity [49,53]. In our study, we observed a notable increase in the abundance of *A. muris* following the induction of colitis, which was effectively mitigated by AE treatment, restoring its levels to normal. This indicates a potential role of AE in attenuating colitis by influencing the abundance of specific bacterial species, such as *A. muris*.

Our study had some limitations. Most notably, it relied solely on animal models to assess the therapeutic potential of AE in IBD. Although murine models provide valuable insights into disease mechanisms and potential treatments, the findings from animal studies may not always directly translate into human outcomes. Therefore, caution should be exercised when extrapolating these results to human populations, and further preclinical studies in diverse animal models, as well as human clinical trials, are necessary to validate the efficacy and safety of AE in treating IBD. To address this limitation and enhance the translational relevance of these findings, future research should focus on conducting well-designed human clinical trials to evaluate the therapeutic efficacy of AE in treating patients with IBD. These trials should include diverse patient populations to assess the effectiveness of treatments across different disease severities and demographic characteristics. In addition, mechanistic studies exploring the specific molecular pathways underlying the therapeutic effects of AE in IBD should be conducted to further elucidate its mode of action and optimize treatment strategies. Such research will contribute to the development of evidence-based therapies for IBD that can improve patient outcomes and quality of life.

In conclusion, AE holds great promise as a natural remedy for IBD, offering a multifaceted approach for the treatment of inflammation, oxidative stress, and dysbiosis in the gut microbiota. Further research is warranted to fully elucidate the therapeutic mechanisms of AE and to optimize its clinical application in the management of IBD and other inflammatory diseases.

Ethical approval

The animal experimental protocols were approved by the Animal Ethics Committee of The First People's hospital of Lianyungang (approval No. KD07230005).

Consent to publish

All authors gave final approval of the version to be published.

Table 6
The mRNA level of IL-4 and IL-13 in control, DSS and DSS + AE group.

	Control	DSS	DSS + AE
IL-4	1.00 ± 0.09	4.37 ± 0.49	2.30 ± 0.31
P value		0.000	0.003
IL-13	1.00 ± 0.11	3.26 ± 0.33	1.71 ± 0.09
		0.000	0.001

Table 7
Table of weight changes in control, DSS, pcDNA-NC, pcDNA-NC + AE and pcDNA-IL-4+AE group (g).

	Control	DSS	pcDNA-NC	pcDNA-NC + AE	pcDNA-IL-4+AE
1 day	18.3 ± 0.1	18.4 ± 0.1	18.59 ± 0.14	18.82 ± 0.02	18.52 ± 0.03
3 day	18.5 ± 0.1	18.5 ± 0.2	18.84 ± 0.33	18.91 ± 0.05	18.66 ± 0.05
5 day	18.7 ± 0.1	18.6 ± 0.2	18.84 ± 0.40	18.64 ± 0.06	18.41 ± 0.16
7 day	18.9 ± 0.1	18.4 ± 0.2	18.52 ± 0.42	18.40 ± 0.13	18.15 ± 0.21
9 day	19.1 ± 0.1	18.4 ± 0.2	18.30 ± 0.35	18.52 ± 0.28	17.99 ± 0.15
11 day	19.3 ± 0.1	18.1 ± 0.2	18.06 ± 0.14	18.62 ± 0.20	18.03 ± 0.13
13 day	19.5 ± 0.1	18.0 ± 0.2	17.99 ± 0.27	18.71 ± 0.27	18.11 ± 0.10
15 day	19.7 ± 0.1	17.6 ± 0.2	17.51 ± 0.31	18.80 ± 0.25	18.11 ± 0.07
P value				0.005	0.009

Availability of data and materials

The data that support the findings of this study are available from the corresponding author upon reasonable request.

Funding

This work was supported by the Lianyungang Traditional Chinese Medicine Science and Technology Development Plan Project (No: YB202215).

CRediT authorship contribution statement

Dong Yang: Supervision, Project administration, Data curation. **Tingrui Ge:** Formal analysis, Data curation, Conceptualization. **Jingyi Zhou:** Writing – review & editing, Writing – original draft, Project administration. **Huazhuan Li:** Visualization, Validation, Resources. **Yonggang Zhang:** Writing – original draft, Methodology, Formal analysis.

Declaration of competing interest

The authors declare the following financial interests/personal relationships which may be considered as potential competing interests: Dong Yang reports financial support was provided by Lianyungang Traditional Chinese Medicine Science and Technology Development Plan Project. If there are other authors, they declare that they have no known competing financial interests or personal relationships that could have appeared to influence the work reported in this paper.

Acknowledgment

Not applicable.

References

[1] M. Agrawal, et al., Approach to the management of recently diagnosed inflammatory bowel disease patients: a user's guide for adult and pediatric gastroenterologists, Gastroenterology 161 (1) (2021) 47–65.
[2] S. Coward, et al., The 2023 impact of inflammatory bowel disease in Canada: epidemiology of IBD, J Can Assoc Gastroenterol 6 (Suppl 2) (2023) S9–s15.
[3] G.R. Jones, et al., IBD prevalence in Lothian, Scotland, derived by capture-recapture methodology, Gut 68 (11) (2019) 1953–1960.
[4] G.G. Kaplan, The global burden of IBD: from 2015 to 2025, Nat. Rev. Gastroenterol. Hepatol. 12 (12) (2015) 720–727.
[5] C.P. Selinger, K. Rosiou, M.V. Lenti, Biological therapy for inflammatory bowel disease: cyclical rather than lifelong treatment? BMJ Open Gastroenterol 11 (1) (2024).
[6] S.C. Shah, S.H. Itzkowitz, Colorectal cancer in inflammatory bowel disease: mechanisms and management, Gastroenterology 162 (3) (2022) 715–730.e3.
[7] H. Everhov A, et al., Inflammatory bowel disease and pancreatic cancer: a Scandinavian register-based cohort study 1969-2017, Aliment. Pharmacol. Ther. 52 (1) (2020) 143–154.
[8] Q. Guan, A comprehensive review and update on the pathogenesis of inflammatory bowel disease, J Immunol Res 2019 (2019) 7247238.
[9] S. Jarmakiewicz-Czaja, et al., Genetic and epigenetic etiology of inflammatory bowel disease: an update, Genes 13 (12) (2022).
[10] Q. Hou, et al., Intestinal stem cells and immune cell relationships: potential therapeutic targets for inflammatory bowel diseases, Front. Immunol. 11 (2020) 623691.

[11] L.N. Zaripova, et al., Mesenchymal stem cells in the pathogenesis and therapy of autoimmune and autoinflammatory diseases, Int. J. Mol. Sci. 24 (22) (2023).
[12] Y. Pan, et al., The protective and pathogenic role of Th17 cell plasticity and function in the tumor microenvironment, Front. Immunol. 14 (2023) 1192303.
[13] R. Gomez-Bris, et al., CD4 T-cell subsets and the pathophysiology of inflammatory bowel disease, Int. J. Mol. Sci. 24 (3) (2023).
[14] Y. Ma, et al., Metagenome analysis of intestinal bacteria in healthy People, patients with inflammatory bowel disease and colorectal cancer, Front. Cell. Infect. Microbiol. 11 (2021) 599734.
[15] J. Park, J.H. Cheon, Updates on conventional therapies for inflammatory bowel diseases: 5-aminosalicylates, corticosteroids, immunomodulators, and anti-TNF-α, Korean J Intern Med 37 (5) (2022) 895–905.
[16] S. Yuan, et al., Traditional Chinese medicine and natural products: potential approaches for inflammatory bowel disease, Front. Pharmacol. 13 (2022) 892790.
[17] T. Wang, et al., Traditional Chinese medicine treats ulcerative colitis by regulating gut microbiota, signaling pathway and cytokine: future novel method option for pharmacotherapy, Heliyon 10 (6) (2024) e27530.
[18] Q. Cai, L. Wu, Y. Zhou, Experiences with traditional Chinese medicine among patients with inflammatory bowel disease: a qualitative study, Gastroenterol. Nurs. 43 (2) (2020) 135–145.
[19] Z. Yang, et al., A potential therapeutic target in traditional Chinese medicine for ulcerative colitis: macrophage polarization, Front. Pharmacol. 13 (2022) 999179.
[20] M. Zhu, et al., Exploring the mechanism of aloe-emodin in the treatment of liver cancer through network pharmacology and cell experiments, Front. Pharmacol. 14 (2023) 1238841.
[21] X. Dong, et al., Aloe-emodin: a review of its pharmacology, toxicity, and pharmacokinetics, Phytother Res. 34 (2) (2020) 270–281.
[22] G. Şeker Karatoprak, et al., Advances in understanding the role of aloe emodin and targeted drug delivery systems in cancer, Oxid. Med. Cell. Longev. 2022 (2022) 7928200.
[23] H. Gao, Y. Ren, C. Liu, Aloe-emodin suppresses oxidative stress and inflammation via a PI3K-dependent mechanism in a murine model of sepsis, Evid Based Complement Alternat Med 2022 (2022) 9697887.
[24] Y. Hu, et al., Assessment of the anti-inflammatory effects of three rhubarb anthraquinones in LPS-Stimulated RAW264.7 macrophages using a pharmacodynamic model and evaluation of the structure-activity relationships, J. Ethnopharmacol. 273 (2021) 114027.
[25] M. Iwaszko, S. Biały, K. Bogunia-Kubik, Significance of interleukin (IL)-4 and IL-13 in inflammatory arthritis, Cells 10 (11) (2021).
[26] J.K. Nguyen, et al., The IL-4/IL-13 axis in skin fibrosis and scarring: mechanistic concepts and therapeutic targets, Arch. Dermatol. Res. 312 (2) (2020) 81–92.
[27] J. Melo-Cardenas, et al., IL-13/IL-4 signaling contributes to fibrotic progression of the myeloproliferative neoplasms, Blood 140 (26) (2022) 2805–2817.
[28] A. Le Floc'h, et al., Dual blockade of IL-4 and IL-13 with dupilumab, an IL-4Rα antibody, is required to broadly inhibit type 2 inflammation, Allergy 75 (5) (2020) 1188–1204.
[29] Q. D'Arcy, et al., The IL-4/IL-13 signaling axis promotes prostatic fibrosis, PLoS One 17 (10) (2022) e0275064.
[30] L. Yang, et al., METTL3 overexpression aggravates LPS-induced cellular inflammation in mouse intestinal epithelial cells and DSS-induced IBD in mice, Cell Death Dis. 8 (1) (2022) 62.
[31] I. Bakke, et al., Mucosal and faecal neutrophil gelatinase-associated lipocalin as potential biomarkers for collagenous colitis, J. Gastroenterol. 56 (10) (2021) 914–927.
[32] J. Su, et al., Aloe-emodin ameliorates cecal ligation and puncture-induced sepsis, Int. J. Mol. Sci. 24 (15) (2023).
[33] K. Sun, et al., Antitumor effects of Chinese herbal medicine compounds and their nano-formulations on regulating the immune system microenvironment, Front. Oncol. 12 (2022) 949332, https://doi.org/10.3389/fonc.2022.949332.
[34] B. Hu, et al., Aloe-emodin from rhubarb (Rheum rhabarbarum) inhibits lipopolysaccharide-induced inflammatory responses in RAW264.7 macrophages, J. Ethnopharmacol. 153 (3) (2014) 846–853.
[35] S. Ashique, et al., Recent updates on correlation between reactive oxygen species and synbiotics for effective management of ulcerative colitis, Front. Nutr. 10 (2023) 1126579.
[36] R. Gao, et al., Emodin improves intestinal health and immunity through modulation of gut microbiota in mice infected by pathogenic Escherichia coli O(1), Animals (Basel) 11 (11) (2021).
[37] F. Crouwel, H.J.C. Buiter, N.K. de Boer, Gut microbiota-driven drug metabolism in inflammatory bowel disease, J Crohns Colitis 15 (2) (2020) 307–315.
[38] Y. Zhou, D. Wang, W. Yan, Treatment effects of natural products on inflammatory bowel disease in vivo and their mechanisms: based on animal experiments, Nutrients 15 (4) (2023).
[39] S. Yang, et al., Aloin reduces HMGB1-mediated septic responses and improves survival in septic mice by activation of the SIRT1 and PI3K/Nrf2/HO-1 signaling Axis, Am. J. Chin. Med. 47 (3) (2019) 613–633.
[40] S. Staffieri, et al., Aloe-emodin overcomes anti-cancer drug resistance to temozolomide and prevents colony formation and migration in primary human glioblastoma cell lines NULU and ZAR 28 (16) (2023) 6024.
[41] T. Hussain, et al., Aloe-emodin exhibits growth-suppressive effects on androgen-independent human prostate cancer DU145 cells via inhibiting the Wnt/β-catenin signaling pathway: an in vitro and in silico study 14 (2024).
[42] He, M.T., et al., Aloe-emodin isolated from rheum undulatum L. Regulates cell cycle distribution and cellular senescence in human prostate cancer LNCaP cells. J. Diet. Suppl.: p. 1-19.
[43] N. Yan, et al., Neuroprotective effect of aloe emodin against Huntington's disease-like symptoms in R6/1 transgenic mice, Food Funct. 14 (11) (2023) 5205–5216.
[44] A. Gunaydin-Akyildiz, et al., Emodin and aloe-emodin, two potential molecules in regulating cell migration of skin cells through the MAP kinase pathway and affecting Caenorhabditis elegans thermotolerance, BMC Molecular and Cell Biology 24 (1) (2023) 23.
[45] Y. Xie, et al., Antimicrobial efficacy of aloe-emodin mediated photodynamic therapy against antibiotic-resistant Pseudomonas aeruginosa in vitro, Biochem. Biophys. Res. Commun. 690 (2024) 149285.
[46] Y. Chen, et al., Aloe emodin reduces cardiac inflammation induced by a high-fat diet through the TLR4 signaling pathway, Mediat. Inflamm. 2020 (2020) 6318520.
[47] Y. Ma, et al., Aloin suppresses lipopolysaccharide-induced inflammation by inhibiting JAK1-STAT1/3 activation and ROS production in RAW264.7 cells, Int. J. Mol. Med. 42 (4) (2018) 1925–1934.
[48] J. Zhong, et al., Aloin attenuates cognitive impairment and inflammation induced by d-galactose via down-regulating ERK, p38 and NF-κB signaling pathway, Int. Immunopharm. 72 (2019) 48–54.
[49] N. Pfeiffer, et al., Acetatifactor muris gen. nov., sp. nov., a novel bacterium isolated from the intestine of an obese mouse, Arch. Microbiol. 194 (11) (2012) 901–907.
[50] C. Lee, et al., CD1d modulates colonic inflammation in NOD2-/- mice by altering the intestinal microbial composition comprising Acetatifactor muris, J Crohns Colitis 13 (8) (2019) 1081–1091.
[51] K. Wang, et al., Bifidobacterium longum R0175 protects rats against d-galactosamine-induced acute liver failure, mSphere 5 (1) (2020).
[52] R. Kübeck, et al., Dietary fat and gut microbiota interactions determine diet-induced obesity in mice, Mol. Metabol. 5 (12) (2016) 1162–1174.
[53] K. Weitkunat, et al., Short-chain fatty acids and inulin, but not guar gum, prevent diet-induced obesity and insulin resistance through differential mechanisms in mice, Sci. Rep. 7 (1) (2017) 6109.